On x-ray channelling in microcapillaries and nanocapillaries

2003 J. Phys.: Condens. Matter 15 3171

(http://iopscience.iop.org/0953-8984/15/19/317)

INSTITUTE OF PHYSICS PUBLISHING JOURNAL OF PHYSICS: CONDENSED MATTER

J. Phys.: Condens. Matter **15** (2003) 3171–3180 PII: S0953-8984(03)59316-X

On x-ray channelling in microcapillaries and nanocapillaries

S Bellucci [1,3] **and S B Dabagov**[1,2]

[1] INFN—Laboratori Nazionali di Frascati, PO Box 13, I-00044, Frascati, Italy
[2] RAS—P N Lebedev Physical Institute, 119991 Moscow, Russia

E-mail: bellucci@lnf.infn.it

Received 6 February 2003
Published 6 May 2003
Online at stacks.iop.org/JPhysCM/15/3171

Abstract

In this work, x-ray propagation in microsize and nanosize capillaries has been considered in the framework of a simple unified wave theory. It is shown that diminishing of the channel sizes completely changes the mode of beam transportation; that is, we obtain the transformation of surface channelling in microcapillaries to bulk channelling in nanocapillaries (nanotubes).

1. Introduction

Nowadays, capillary optics represents a well-established x-ray and neutron optical instrument that allows experiments to be performed quite efficiently on a much smaller scale than with conventional x-ray devices. These optical elements consist of hollow tapered tubes that condense neutral particles by multiple reflections from the inner channel surface [1, 2]. Moreover, capillary optics can also rely on the ability of a tapered and/or bent capillary channel to act as an x-ray waveguide [3]; in other words, an optical element may be considered as a whispering-gallery x-ray device.

As is well known, a whispering gallery device is a multiple-reflection one with a large number of bounces [4]. The total subtended angular aperture of the device is determined by the number of bounces N and the glancing angle θ, and equals $2N\theta$. While the reflectivity of single-bounce light from a substance with the complex dielectric function $\varepsilon = 1 - \delta + \mathrm{i}\beta$ (δ and β are the parameters of polarizability and attenuation, respectively) is defined by

$$R_{1\{\substack{s\\p}\}} \simeq 1 - 2\theta\,\mathrm{Re}\left(\left\{\begin{array}{c}1\\ \varepsilon\end{array}\right\}(\varepsilon - 1)^{-1/2}\right), \tag{1}$$

where s, p are the indices for the radiation polarization, the integral reflection may be estimated by taking the $\theta \to 0$ ($N \to \infty$) limit

$$R_{\{\substack{s\\p}\}} \simeq \exp(-(1 - R_{1\{\substack{s\\p}\}})N). \tag{2}$$

[3] Author to whom any correspondence should be addressed.

Evaluations made using these relations have shown that the whispering galleries offer high efficiency with narrow bandpass [5].

Application of wave theory to the passage of radiation through capillary structures opens up new prospects for study [6–8]. As will be shown below, capillary optical systems act in such a way that radiation propagating in channels consists of two portions: one is scattered by the laws of ray optics; the other is captured in bound modes by a surface potential. Moreover, when the channel size values approach the transverse wavelength of radiation, the bulk channelling of photons occurs similarly to the channelling of charged particles in crystals [9]. Now, the technology of capillary system manufacture allows structures at the deep submicron level to be produced [10]. For example, as samples for examination one may consider carbon nanostructures (nanocapillary systems) [11], in whose fabrication major progress has been achieved in recent years [12].

A graphitic nanotube [13–15] may be considered as a small-size (nanosize) capillary. Its wall is formed of carbon atoms, the distance between which is estimated to be about 1–2 Å. The typical diameter of a single nanotube is tens of nanometres (the channel diameter/wall thickness ratio may reach two orders of magnitude), and the length of such a structure may be of submillimetre order. All these features of the nanotube structures result in the utilization of wave propagation theory instead of ray approximation theory; consequently, nanotubes may be considered as x-ray waveguides. This allows the well-known channelling theory to be applied for describing x-ray beam propagation inside these structures [16, 17].

Following recent developments in studying the properties of nanostructured materials [18–21], also simulations of particle beam channelling in carbon nanotubes have been performed, in order to evaluate the possibilities for experimental observation of channelling effects in both straight and bent nanotubes, considering different charged particle species, such as protons of 1.3 and 70 GeV, and positrons of 0.5 GeV [22]. There, the capabilities of a nanotube channelling technique for charged particle beam steering were discussed, on the basis of earlier Monte Carlo simulations [23]. In the present work, a unified description of x-ray propagation (note that the same theory is valid for neutrons) through capillaries of various diameters is presented.

2. Quantum–wave dualism

As has been shown recently, the propagation of x-ray photons through capillary systems exhibits a rather complex character [24]. Not all features shown in the experiments can be explained within the geometrical (ray) optics approximation [25–27]. In contrast, the application of wave optics methods allows us to describe in detail the processes of radiation spreading into capillaries.

The propagation of x-radiation through capillary systems is mainly governed by its interaction with the inner channel walls. In the ideal case, when the boundary between the hollow capillary and the walls is a smooth edge, the beam is split into two components: the mirror-reflected and refracted ones. The latter appear sharply suppressed in the case of total external reflection. The characteristics of scattering inside capillary structures can be evaluated from the solution of a wave propagation equation. In the first-order approximation, without taking into account the roughness correction $\Delta\varepsilon(\boldsymbol{r}) = 0$ ($\Delta\varepsilon$ is the perturbation in dielectric permittivity induced by the presence of roughness), the wave equation in the plane transverse to the propagation direction reads

$$(\nabla_\perp^2 - k^2\delta(r_\perp) + k_\perp^2)E(r_\perp) = 0, \tag{3}$$

where E is a radiation field function, and $\boldsymbol{k} \equiv (k_\parallel, k_\perp)$ is a wavevector.

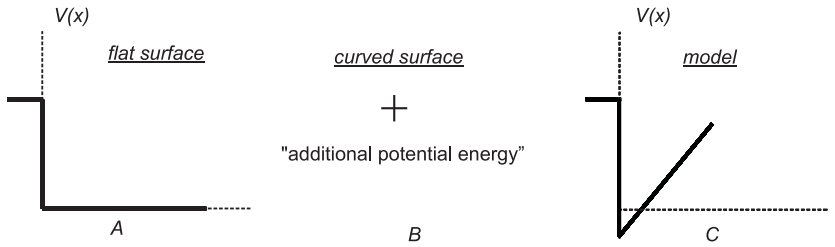

Figure 1. The change of the interaction potential between the flat surface (A) and the curved one (B). For simplicity, in calculations the 'real potential' (B) may be replaced by the model potential (C).

Because the transverse wavevector may be presented as $k_\perp \approx k\theta$ for grazing incidence ($\theta \ll 1$), an 'effective interaction potential' can be estimated by the expression

$$V_{eff}(\boldsymbol{r}_\perp) = k^2(\delta(r_\perp) - \theta^2) = \begin{cases} -k^2\theta^2, & r_\perp < r_1, \\ k^2(\delta_0 - \theta^2), & r_\perp \geqslant r_1, \end{cases} \tag{4}$$

where r_1 corresponds to the reflecting wall position. From the latter, the phenomenon of total external reflection at $V_{eff} = 0$ follows, when $\theta \equiv \theta_c \simeq \sqrt{\delta_0}$—Fresnel's angle.

When we introduce a curvature in the reflecting surface, the effective potential obtains an additional contribution. This term, which corresponds to the additional 'potential energy', can be seen physically in the following way. Due to the reflecting surface curvature at the angle φ, the photon receives an angular momentum $kr_{curv}|_\varphi$, where r_{curv} is the curvature radius of the photon trajectory, φ is an azimuthal angle in the cylindrical coordinates chosen along the direction of radiation propagation (in the case of a capillary, i.e. a cylindrical tube, the direction of propagation cannot coincide with the main z-axis of a cylinder, $\widehat{(\boldsymbol{k}, \boldsymbol{e}_z)} \neq 0$). The latter gives the contribution to the effective potential as the 'centrifugal potential energy' $-2k^2r_\perp/(r_{curv})$ term

$$V_{eff}(r_\perp) = k^2\left(\delta(r_\perp) - \theta^2 - 2\frac{r_\perp}{r_{curv}}\right). \tag{5}$$

The expression for the interaction potential in the case of a flat surface, equation (4), clearly follows the most general expression (5) for a curved surface when the curvature radius $r_{curv} \to \infty$. The change in shape of the potential is explained by the scheme in figure 1. Because of the variation in the spatial system parameters, the interaction potential has been changed from the step potential with the potential barrier of $k^2\delta_0$ to a well potential with its depth and width defined by the channel characteristics. Moreover, increase in the curvature leads to broadening of the potential well that, in turn, translates to an increase in number of the bound states. So, for small slope of the potential the wave features of the radiation scattering from the surface become negligible, and a problem of radiation propagation can be solved in the framework of the ray approach.

In the following we briefly discuss a solution of the wave equation in the case of an ideal reflecting surface (i.e. without roughness), when the reflected beam is basically determined by the coherently scattered part of the radiation (for details see [28, 29]). The evaluation of the wave equation with the boundary conditions of a capillary channel shows that x-radiation may be distributed over the bound state modes defined by the capillary channel potential (see below). It is important to underline here that the channel potential acts as an effective reflecting barrier, and then an effective transmission of x-radiation by the hollow capillary tubes is observed. While the main part of the radiation undergoes incoherent diffuse scattering [30], the remaining

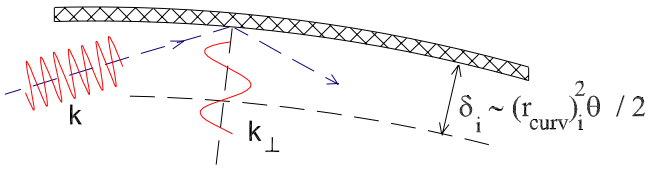

Figure 2. An illustration of x-ray reflection from the inner capillary surface. At glancing angles θ, when the width of a beam $\delta_i(\theta)$ becomes comparable with the transverse wavelength $\lambda_\perp(\theta)$, the radiation is grasped in a mode of surface channelling.

(This figure is in colour only in the electronic version)

contribution (usually small) is due to coherent scattering that represents a special phenomenon, extremely interesting to observe and clarify [31].

Let us estimate the upper limit of the curvature radius $(r_{curv})_{max}$ (which is defined as capillary/system for capillaries bending and/or by the radiation propagation trajectory), at which the wave behaviours are displayed under propagation of radiation in channels [6], by considering a photon with the wavevector $\boldsymbol{k}$ channelling into a capillary with curvature radius $(r_{curv})_i$ (the ith trajectory is chosen to coincide with the direction of radiation propagation $\boldsymbol{k}$). At small glancing angles, θ, the change of the longitudinal (along the propagation direction) wavevector, $k_\parallel$, under reflection from the capillary wall is negligibly small; mainly one changes the transverse wavevector, $k_\perp$:

$$k_\perp \simeq k\theta \qquad (\theta < \theta_c). \tag{6}$$

Correspondingly, from this relation it follows that the transverse wavelength will far exceed the longitudinal wavelength. This makes the interference effects observable even for very short wavelengths. Indeed, for

$$\lambda_\perp = \lambda/\theta \gg \lambda, \tag{7}$$

quantum mechanical principles say that, in order to display the wave properties of a channelling photon, it is necessary that typical sizes of an 'effective channel' δ_i, in which waves have been propagating, be comparable to the transverse wavelength, i.e. $\delta_i(\theta) \simeq \lambda_\perp(\theta)$ (figure 2). Taking into account the fact that the term for δ_i is defined by the ith layer curvature radius $(r_{curv})_i$ and the incidence angle θ—that is, $\delta_i \simeq (r_{curv})_i\theta^2/2$—this condition may be rewritten in the following form:

$$(r_{curv})_i\theta^3 \sim \lambda, \tag{8}$$

from which we obtain $(r_{curv})_{max} \sim 10$ cm for a photon of $\lambda \sim 1$ Å wavelength at glancing angle $\theta \simeq \theta_c/3$. So, from this simple estimate we can conclude that the relation (8) provides a specific dependence for surface bound state propagation of x-rays—surface channelling—along the curved surfaces (for instance, in microcapillary systems; see also [32]).

3. Propagation equation

3.1. Surface channelling

Since the waveguide is a hollow cylindrical tube, if the absorption is considered to be negligible, the interaction potential, in which a wave propagates, is determined by equation (5) with the radiation polarizability parameter $\delta_0 \simeq \theta_c^2$. We solve the wave equation in normalized cylindrical coordinates $\boldsymbol{r} \equiv (r_\perp, \varphi, z)$ for the purpose of dealing with dimensionless variables. Since we are mainly interested in the surface propagation, we choose a reference frame with the

z-axis oriented along the direction of propagation. The solution that we are seeking describes the propagation of waves near the surface of the reflecting wall $r_\perp \simeq r_1$, which, in fact, defines a waveguiding character along the trajectory of the curvature radius r_1. Hence, we consider the approximation $r_\perp = r_1 - \rho$, $|\rho| \ll r_1$ along the trajectory for a given propagation mode m. The range of values for the curvature radius reads $r_0 \leqslant r_1 \leqslant r_{bend}$, where the extreme cases correspond to the proper channel radius r_0 and to the bending curvature of the channel as a whole r_{bend}. This method has the advantage of simplifying the mathematical treatment, allowing us to restrict our consideration to just the radial equation of motion. In terms of the solution of the latter $u_m(\rho)$, the general solution reads

$$E_n \simeq \sum_m C_m u_m(\rho) \mathrm{e}^{\mathrm{i}(k_\parallel z + n\varphi)},$$
$$u_m(\rho) \propto \begin{cases} \mathrm{Ai}(\rho + \rho_m), & \rho > 0 \\ \alpha\, \mathrm{Ai}'(\rho_m)\mathrm{e}^{\alpha\rho}, & \rho < 0\ (\alpha > 0) \end{cases} \tag{9}$$

where the prime denotes differentiation with respect to x, $\mathrm{Ai}(x)$ is the Airy function, satisfying an equation $\mathrm{Ai}''(x) = x\,\mathrm{Ai}(x)$ and decaying exponentially at $x > 0$, ρ_m is the mth zero of the Airy function, and $\alpha = \delta_0^{-1/2}(\frac{2}{kr_1})^{1/3}$ (the method used was described in detail in previous publications; see, for example, [8]). Evidently, these expressions are valid only for the lower-order modes and in the vicinity of a channel surface. The expression (9) characterizes the waves that propagate close to the waveguide wall or, in other words, the equation describes the grazing modal structure of the electromagnetic field inside a capillary (surface bound x-ray channelling states; figure 3). The solution shows also that the wavefunctions are exponentially damped both inside the channel wall: $\rho < 0$ (as $\mathrm{e}^{-2|\alpha||\rho|}$), and going from the wall towards the centre: $\rho > 0$ (as the Airy function decays). It should be underlined here that the bound modal propagation in the hollow part of the system takes place without wavefront distortion. The analysis of these expressions allows us also to conclude that almost all radiation power is concentrated in the hollow region and, as a consequence, a small attenuation along the waveguide walls is observed.

As for the supported modes of the electromagnetic field, estimating a characteristic radial size of the main grazing mode ($m = 0$) results in

$$\bar{u}_0 \simeq 0.75\left(\frac{\lambda^2 r_1}{\pi^2}\right)^{1/3}, \tag{10}$$

and we can conclude that the typical radial size $\bar{u}_0$ may significantly exceed the wavelength λ, whereas the curvature radius r_1 in the trajectory plane exceeds the inner channel radius, r_0: $\bar{u}_0 \gg \lambda$. For example, at the radiation wavelength $\lambda = 10$ Å an estimation of the characteristic size $\bar{u}_0$ in the extreme case, when $r_1 \simeq r_0$, gives us that $\bar{u}_0 \gtrsim 75$ Å for a capillary channel with the radius $r_0 = 10\ \mu$m.

3.2. Bulk channelling

Above, we have considered the transmission of x-ray beams by capillary systems of micron- and submicron-size channels. Obviously, in that case we deal with surface channelling of radiation, due to the channel sizes being larger than the radiation wavelength by at least three orders of magnitude and the bounding happens due to the surface curvature. However, the situation varies sharply in the case where the sizes of channels become comparable with the radiation wavelength. In practice this means that the angle of diffraction for the given wave, determined as $\theta_d = \lambda/d$ (where d is a capillary diameter), becomes comparable with a critical angle of total external reflection. In other words, the transverse wavelength of a photon

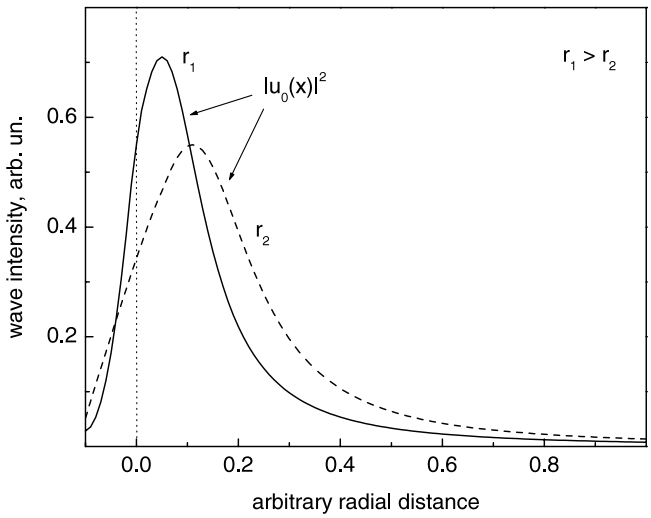

Figure 3. The radial distributions of the main bound mode of radiation inside a capillary channel for two different channel radii, $(r_0)_1$ and $(r_0)_2$ (the curvature radius has been chosen to be the extreme case: $r_1 = r_0$). The decrease in diameter results in a spatial displacement of the distribution away from the channel wall towards the centre. The wall surface position is shown by the dotted line.

approaches the diameter of a capillary: $\lambda_\perp/d \sim 1$. When considering bulk channelling, as opposed to the surface channelling case, in the first approximation, for small slope of the potential due to the curvature, we can ignore the contribution of the longitudinal curvature. In this case, channelling of photons (note: not superficial/surface channelling!) in channels of capillary systems should occur even in the absence of curvature; i.e. we actually deal with an x-ray waveguide optics similar to the light waveguide one. Moreover, under the condition of ordering of channels in the system cross-section, the capillary nanostructures are similar to crystals, as seen from charged particles going through them at small angles to the main crystallographic directions [16, 17].

As the analysis of the wave equation shows, the problem cannot be analytically resolved for the real nanotube potential. For the sake of simplicity, let us consider the problem in the radial (along the r-axis, transverse to the z-axis) approximation for the periodic field of a multilayer waveguide with size d_0 of the central channel and distance d between the layers composing the waveguide wall. The interaction potential of the radiation in such a waveguide system may be presented as follows:

$$V(r) = \sum_n V_n(r) = k_r^2\left[-1 + \Delta \sum_n \delta\left(|r| - \frac{d_0}{2} - nd\right)\right], \tag{11}$$

where $\Delta \equiv \bar{\delta}_0 d$ is the spatially averaged polarizability of the wall substance, $k_r^2 = k^2 - k_z^2$, and $\delta(x)$ is the δ-function for the argument x. Such simplification allows us to emphasize that bulk channelling takes place even in a planar waveguide with narrow 'hollow' channels.

Taking into account the boundary conditions and because of the potential symmetry, one may conclude that for the central nanotube channel $|r| \leqslant d_0/2$, the solution of the propagation equation in the transverse plane will be defined by the simple expression

$$E_0(r) = \begin{cases} a\cos(k_r r), & \text{even mode,} \\ a\sin(k_r r), & \text{odd mode.} \end{cases} \tag{12}$$

Then we define the equation solution for the first layer $d_0/2 \leqslant |r| \leqslant d_0/2+d$ by superposition of the oppositely directed waves $E(r) = b\mathrm{e}^{\mathrm{i}k_r r} + c\mathrm{e}^{-\mathrm{i}k_r r}$. As has been done in the previous section, we make the mathematical assumption that all the modes of the total energy operator constitute a complete set of functions in the sense that an arbitrary continuous function can be expanded in terms of them. Then, we have a wavefunction $E(r)$ at a particular instant in time that obeys the continuous boundary conditions at the walls.

Due to the fact that the potential (11) is periodic: $V(r) = V(r+d)$, the last solution should be governed by Bloch's theorem: $E(r+d) = \mathrm{e}^{\mathrm{i}\varkappa d}E(r)$, where $\varkappa$ is the complex quasimomentum: $\varkappa \equiv \operatorname{Im}\varkappa$. So, taking into account this fact and solving a wave equation with the boundary conditions

$$\begin{aligned} &E\left(\frac{d_0}{2}+d\right) = \mathrm{e}^{\mathrm{i}\varkappa d}E\left(\frac{d_0}{2}\right), \\ &E'_r\left(\frac{d_0}{2}+d\right) = \mathrm{e}^{\mathrm{i}\varkappa d}E'_r\left(\frac{d_0}{2}+0\right) - k^2\Delta E\left(\frac{d_0}{2}+d\right), \end{aligned} \tag{13}$$

one can write the following expression for the parameter $\varkappa$:

$$\mathrm{e}^{2\mathrm{i}\varkappa d} - 2\left(\cos(k_r d) - \frac{k^2\Delta}{k_r}\sin(k_r d)\right)\mathrm{e}^{\mathrm{i}\varkappa d} + 1 = 0. \tag{14}$$

Correspondingly, matching the solutions for the wavefunction and its derivative at the plane $|r| = \frac{d_0}{2}$, we obtain the dispersion relations for even and odd channelling waves:

$$\begin{aligned} \tan\frac{k_r d_0}{2} &= -\frac{k^2\Delta}{k_r} + \frac{\cos(k_r d) - \mathrm{e}^{\mathrm{i}\varkappa d}}{\sin(k_r d)}, \\ \cot\frac{k_r d_0}{2} &= \frac{k^2\Delta}{k_r} - \frac{\cos(k_r d) - \mathrm{e}^{\mathrm{i}\varkappa d}}{\sin(k_r d)}, \end{aligned} \tag{15}$$

which allow the eigenvalue/eigenfunction problem to be solved. These relations describe completely the problem of transport of radiation both for the presence of a channel $d_0 \gg d$ and for the case of a uniform crystal with $d_0 = d$. It is interesting to consider the case of a narrow channel with $\{k_r d_0, k_r d\} \ll 1$, which corresponds to the case of a multiwall nanotube. The wavefunctions of the supported modes in this case are described by the expression

$$E_n(r) \propto \begin{cases} \cos(k_r r)\mathrm{e}^{\mathrm{i}k_z z}, & -\frac{d_0}{2} \leqslant |r| \leqslant \frac{d_0}{2} \\ \cos\dfrac{k_r d_0}{2}\dfrac{\mathrm{e}^{\mathrm{i}\varkappa r}\sin(k_r|\tilde{r}|) - \sin[k_r(|\tilde{r}|-d)]}{\sin(k_r d)} & \\ \quad \times \mathrm{e}^{\mathrm{i}(\varkappa n d + k_z z)}, & \frac{d_0}{2} + nd \leqslant |r| \leqslant \frac{d_0}{2} + (n+1)d, \end{cases} \tag{16}$$

where $|\tilde{r}| \equiv |r| - d_0/2 - nd$. We see that the equations (15) may be solved only for even modes. The solution for an even mode gives us the relation for the quasimomentum:

$$\mathrm{e}^{\mathrm{i}\varkappa d} \simeq 1 - \frac{k^2(d-d_0)}{2}\Delta. \tag{17}$$

The imaginary part of the complex quasimomentum, $\operatorname{Im}\varkappa = \frac{k^2}{2}(1-\frac{d_0}{d})\operatorname{Re}\Delta$, provides a decrease of the modal amplitude with distance from the channel axis. It is important to underline that the even mode exists for any ratio between the channel size and the layer distance, and may be characterized by a reduction of the order of $\frac{k^3}{4}(1-\frac{d_0}{d})^2\operatorname{Re}\Delta\operatorname{Im}\Delta$ in the longitudinal decay parameter $k_z = \sqrt{k^2 - k_r^2}$. The spatial distribution of the mode has a maximum at the centre of the channel, and due to the leak through the potential barrier of wall layers we observe the longitudinal propagation of radiation in the nanotube substance. The radial wavefunction distribution for the case of a system of equidistant layers is shown in

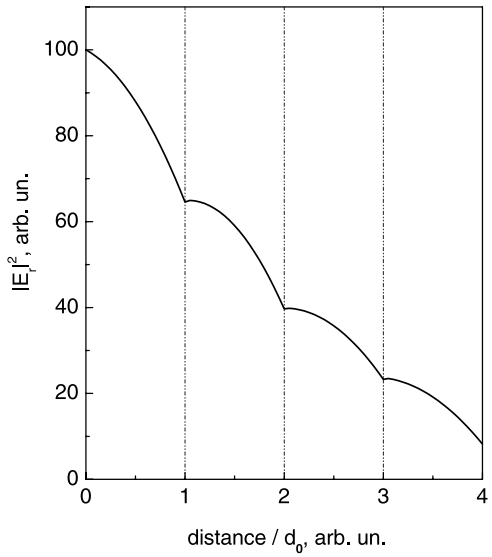

Figure 4. The typical radial wavefunction distribution for a periodic multilayer waveguide, where d is the distance between the layers composing a waveguide wall. An exponential decay $\exp(-|\operatorname{Im}\varkappa|r)$ of the wave with increase in the distance from the channel axis takes place, while some features appear close to the layer walls due to the local maxima of the wavefunctions at these positions.

figure 4. Analysis of the distribution shows an exponential decay $\exp(-|\operatorname{Im}\varkappa|r)$ of the wave with increase in the distance from the nanotube channel axis, while some structures appear close to the nanotube walls due to the local maxima of the wavefunctions at these positions. As seen from expression (17), for a uniform system (without any specified channels—for instance, for crystals) we obtain $\operatorname{Im}\varkappa = 0$, which means that there are no localized modes.

The width of the main mode is defined by the value $|\operatorname{Im}\varkappa|^{-1} \approx$ 100–1000 Å, which may significantly exceed the nanotube channel diameter (less than $\lesssim$100 Å, even in the case of a multiwall nanotube). Because of the small wall thickness of the nanotube channels we have to note that some of the radiation, channelling inside a nanotube structure, will undergo 'tunnelling' through the potential wall barrier. A simple analysis of the radiation propagation in systems shows the presence of the main channelling mode (the main bound state) for any structure, whereas the high modes may be suppressed for specific channel sizes. Hence, nanotubes are of special interest as waveguides, which allow the supported modes to be governed. Moreover, there is special interest in studying the dispersion of radiation in a nanosystem with a multilayered wall. In that case diffraction of waves reflected from various layers of the channel wall should be observed, affecting the radiation distribution at the exit from the system.

4. Conclusions

The reduction in the channel size of capillary structures as well as the discovery of a new class of natural nanosystems—i.e. carbon nanotubes—places the problem of passage of x-ray quanta through these systems on a new level, qualitatively.

In the present work a general unified theory, allowing us to describe processes of radiation passage through capillary systems with a wide range of channel diameters, is presented. Our

analysis shows that in the case of micron diameters the surface channelling of quanta is present in the mechanism of propagation (some of the radiation is distributed, being trapped by the bent surface of the channel). This can crucially influence the angular radiation distribution behind capillary systems. A decrease in size down to the nanolevel results in a transition from surface channelling to bulk channelling. Thus, all radiation is involved in the process of modal propagation, as opposed to the case for surface channelling, where only some of the radiation exhibits bound motion.

Recently, it has been demonstrated that for specific cases a decrease in the angular divergence of the x-radiation after passing through capillary systems may be observed [33]. We have found strong differences between the observed and expected full width at half-maximum (FWHM) values. From the general ray approach estimations, a FWHM value of at least $2\theta_c \simeq 0.9^\circ$ for 4 keV synchrotron radiation photons is expected. This width exceeds both the experimental ($\mathrm{FWHM}^{SR}_{exp}[4\ \mathrm{keV}] = 0.28^\circ$) and Gaussian fitted ($\mathrm{FWHM}^{SR}_{G}[4\ \mathrm{keV}] = 0.22^\circ$) values. An analogous feature arises also in the case of harder radiation. Such behaviour indicates an essential redistribution of radiation scattered inside the channels. The discrepancy obtained between experimental and theoretical results could not be reproduced within the framework of the ray approximation and may be explained using the wave approach method for describing the angular distribution of the reflected beam.

The main purpose of the present work is fundamental—i.e. to study the processes accompanying the x-ray transmission by capillary structures—besides the well-known fact that capillary optics applications are covering larger and larger areas in x-ray physics and chemistry, biology, and medicine. X-ray and neutron research activities over the last ten years have demonstrated that capillary optics is a powerful instrument for guiding neutral particle beams. Capillary/polycapillary optics can be applied in numerous branches of x-ray research, e.g. spectroscopy, fluorescence analysis, crystallography, imaging techniques, tomography, and lithography [10]. In any case, the interest in coherent effects of the radiation interacting with nanosystems is not limited to fundamental research, owing to the potential technological applications (e.g. in new sources of electromagnetic radiation [34, 35]).

As we have seen, thin films of carbon nanotubes can provide the basis for developing interesting devices connected with photonic band gap guides, which use a similar principle, although at optical frequencies (see the pioneering work [36]). Evidently, the efficiency of nanostructured materials for technological applications has yet to be analysed, independently of the importance of the nanotube x-ray waveguide phenomenon from the fundamental point of view.

Acknowledgments

This work was partly supported by the Italian Research Ministry, National Interest Programme ‘Effetti di spin, interazione e proprietà di trasporto in sistemi elettronici fortemente interagenti a bassa dimensionalità’, the NANO experiment of the Commissione Nazionale V of the Istituto Nazionale di Fisica Nucleare and by the Russian Federation Federal Programme ‘Integration’.

References

[1] Engström P, Larsson S and Rindby A 1991 *Nucl. Instrum. Methods* A **302** 547
[2] Thiel D J, Bilderback D H, Lewis A and Stern E A 1992 *Nucl. Instrum. Methods* A **317** 597
[3] Spiller E and Segmüller A 1974 *Appl. Phys. Lett.* **24** 60
[4] Vinogradov A, Kovalev V, Kozhevnikov I and Pustovalov V 1985 *Sov. Phys.–Tech. Phys.* **30** 335
[5] Smith N V and Howells M R 1994 *Nucl. Instrum. Methods* A **347** 115

[6] Dabagov S B 1992 *Research Report of FIROS (Nalchik, Moscow) for 1992* (in Russian)
[7] Dabagov S B and Kumakhov M A 1995 *Proc. SPIE* **2515** 124
[8] Alexandrov Yu M *et al* 1998 *Nucl. Instrum. Methods* B **134** 174
[9] Lindhard J 1965 *K. Dan. Vidensk. Selsk. Mat.-Fys. Medd.* **34** 1
[10] Kumakhov M A 2000 *Proc. SPIE* **4155** 2
[11] Burattini E and Dabagov S B 2001 *Nuovo Cimento* B **116** 361
[12] Saito R, Dresselhaus G and Dresselhaus M S 1998 *Physical Properties of Carbon Nanotubes* (London: Imperial College Press)
[13] Iijima S 1991 *Nature* **354** 56
[14] Ajayan P M and Iijima S 1993 *Nature* **361** 333
[15] Iijima S and Ichihashi T 1993 *Nature* **363** 603
[16] Zhevago N K and Glebov V I 1998 *Phys. Lett.* A **250** 360
[17] Dedkov G V 1998 *Nucl. Instrum. Methods* B **143** 584
[18] Iijima S 2002 *Appl. Phys. Lett.* **80** 2973
[19] Bockrath M *et al* 1999 *Nature* **397** 598
Yao Z *et al* 1999 *Nature* **402** 273
Bellucci S and Gonzalez J 2000 *Eur. Phys. J.* B **18** 3
Bellucci S and Gonzalez J 2001 *Phys. Rev.* B **64** 201106 (rapid communication)
Bellucci S, Gonzalez J and Onorato P 2003 *Preprint* cond-mat/0302149
Kasumov A Yu *et al* 1999 *Science* **284** 1508
Kociak M *et al* 2001 *Phys. Rev. Lett.* **86** 2416
[20] Ebbesen T W 1996 *Phys. Today* **49** 26
[21] Wu Z Y *et al* 2002 *Appl. Phys. Lett.* **80** 2973
[22] Bellucci S *et al* 2003 *Nucl. Instrum. Methods* B **202** 236 (*Preprint* physics/0208081)
[23] Biryukov V M and Bellucci S 2002 *Phys. Lett.* B **542** 111 (*Preprint* physics/0205023)
[24] Dabagov S B *et al* 1995 *J. Synchrotron. Radiat.* **2** 132
[25] Artemiev N, Artemiev A, Kohn V and Smolyakov N 1998 *Phys. Scr.* **57** 228
[26] Dabagov S B and Marcelli A 1999 *Appl. Opt.* **38** 7494
[27] Kukhlevsky S V *et al* 2000 *Nucl. Instrum. Methods* B **168** 276
[28] Dabagov S B *et al* 1998 *Proc. SPIE* **3444** 486
[29] Dabagov S B *et al* 2000 *Appl. Opt.* **39** 3338
[30] Dabagov S B, Marcelli A, Cappuccio G and Burattini E 2002 *Nucl. Instrum. Methods* B **187** 169
[31] Dabagov S B *et al* 2000 *Proc. SPIE* **4138** 79
[32] Liu Chien and Golovchenko J A 1997 *Phys. Rev. Lett.* **79** 788
[33] Cappuccio G, Dabagov S B, Gramaccioni C and Pifferi A 2001 *Appl. Phys. Lett.* **78** 2822
[34] Bellucci S *et al* 2003 *Phys. Rev. Lett.* **90** 034801 (*Preprint* physics/0208028)
[35] Bellucci S *et al* 2003 *Phys. Rev. ST AB* **6** 033502 (*Preprint* physics/0209057)
[36] Yablonovitch E 1987 *Phys. Rev. Lett.* **58** 2059